Comparison of Three Body Models of Different Complexities in Modelling of Equal-Sized Dipole and Folded Dipole Wearable Passive UHF RFID Tags

Toni Björninen [1]

[1] BioMediTech Institute and Faculty of Biomedical Sciences and Engineering
Tampere University of Technology, Tampere, 33720, Finland
toni.bjorninen@tut.fi

Abstract — We compare the performance of equal-sized dipole and folded dipole wearable passive UHF RFID tags using three different body models for the torso of an adult male: cuboid and anatomical models with and without internal structures. The results show that all models estimate the antenna impedance matching appropriately, but only the anatomical models predict the full spatial coverage of the tags properly. We present a novel metrics for analysing the coverage in simulations and compare the simulated and measured tag read ranges to validate our modelling results.

Index Terms — Dipole, e-textile, folded dipole, human body model, RFID tag, wearable antenna.

I. INTRODUCTION

Body area networks (BAN) have become an important trend in wireless communications and the development of wearable wireless technologies is offering marked benefits to numerous applications, such as medicine and healthcare, wellness and sports, and safety and security. Overall, the development is striving towards wearable intelligence: the body-worn sensing and energy harvesting platforms will provide wireless power and data to the human intranet consisting of implanted and body-worn devices [1–2].

Passive ultra-high frequency (UHF) radio-frequency identification (RFID) inspired technology is a compelling approach to energy- and cost-efficient wireless platforms for the future BANs [3–4]. In addition to identification, this versatile technology is adaptable for the purposes of wireless sensing, for instance [5–7]. Currently, perhaps the biggest challenges in the development of wearable wireless devices are the seamless cloth-integration and reliable and effective optimisation of body-worn antennas. Here, the regular printed circuit board is not a viable approach and thus electrically conductive textiles (e-textiles) where conductive parts are patterned from metal-coated fabrics or embroidered with metal-coated sewing threads, for instance, have gained more attention. In the view of textile-compatible manufacturing, simple uniplanar antennas provide clear benefits over structures with multiple interconnected layers. Still, the presence of the body influences uniplanar antennas more and therefore we must optimise them affixed on a human body model.

The body is an extremely complex platform for electromagnetic modelling in terms of both the structure and materials. Thus, for effective simulation of wearable antennas, we must strike the right balance between complexity and prediction accuracy. In this letter, we address this question in the application of wearable RFID tags by comparing equal-sized tags based on dipole and folded dipole antennas using three different human body models of different complexities.

II. HUMAN BODY MODELS AND SIMULATION RESULTS

Fig. 1 show the tag antennas that we optimised using a simple cuboid body model in [8]. This work presents further analysis and comparison of the tag's performance and spatial coverage in more realistic body models illustrated in Fig. 2. The coordinate systems in Figs. 1–2 coincide and indicate the placement of the tag centred in the upper back at the level of the scapula. We first developed the structured anatomical model by adapting the full ANSYS human body model (adult male) by reducing it to the head and upper torso and then removing internal structures that we did not consider having significant size or were not located near the tag. We modelled the electromagnetic properties of the different tissue types using the four-term Cole-Cole dielectric relaxation model with the model parameters taken from IT'IS library [9]. In case of the solid anatomical model, we assigned the material in the whole body as skin (ε_r=41.4, σ=0.867 S/m at 915 MHz) since it is the tissue type nearest to the tag. Finally, we created the cuboid model by adapting the dimensions of a cuboid to fit the torso in the anatomical models as illustrated in Fig. 2 and assigned the dielectric properties of skin on the cuboid. The antenna substrate was EPDM (Ethylene-Propylene-Diene-Monomer, ε_r=1.26, tanδ = 0.007 at 915

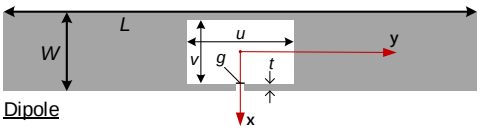

Dipole

t	g	L	W	u	v
2	2	120	20	27	16

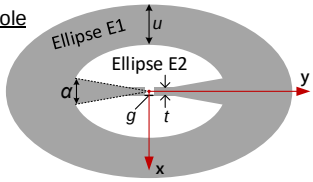

Folded dipole

t	g	α	u	q
2	2	20°	10	1.65

Ellipse	Semi-minor axis	Semi-major axis
E1	$\sqrt{LW/(q\pi)}$	$\sqrt{(qLW)/\pi}$
E2	$\sqrt{LW/(q\pi)}-u$	$\sqrt{(qLW)/\pi}-qu$

Fig. 1. Structural diagrams of the studied antennas.

MHz) cell rubber foam with the thickness of 2 mm and as conductors we used both 20-µm copper foil (conductivity: 58 MS/m) and nickel and copper plated Less EMF Shieldit Super Fabric (sheet resistance: 0.16 Ω/Sq.). The RFID IC we used was NXP UCODE G2iL RFID IC. It has the wake-up power of −18 dBm (15.8 µW) and we modelled it as a parallel connection of the resistance and capacitance of 2.85 kΩ and 0.91 pF, respectively [8].

The main performance indicator of passive tags is the attainable tag read range (d_{tag}) that in passive UHF RFID systems is limited by the tag's capability to harvest energy from the reader's carrier signal. In free space,

$$d_{tag}=\frac{\lambda}{4\pi}\sqrt{\left\{\frac{4\,\mathrm{Re}(Z_A)\,\mathrm{Re}(Z_{IC})}{\left|Z_A+Z_{IC}\right|^2}\right\}\frac{\chi_p e_r D(\theta,\phi)EIRP}{P_{ic0}}}, \quad (1)$$

where λ is the wavelength of the reader's signal, the factor in curly brackets is the antenna-IC power transmission efficiency (τ) determined by the tag antenna and IC impedances Z_A and Z_{IC}, respectively, χ_p is the mutual polarisation loss factor between the tag antenna and the incident wave from the reader, e_r and $D(\theta,\varphi)$ are the radiation efficiency and directivity of the tag antenna, respectively, $EIRP$ is the equivalent isotropically radiated power of the reader, and P_{ic0} is the wake-up power of the tag IC.

The complex electric field vector (**E**) of an electromagnetic wave can be expressed as a sum of orthogonal purely left and right hand circularly polarised components $\mathbf{E}_L$ and $\mathbf{E}_R$, respectively, by introducing a complex scalar (γ) called circular polarisation ratio such

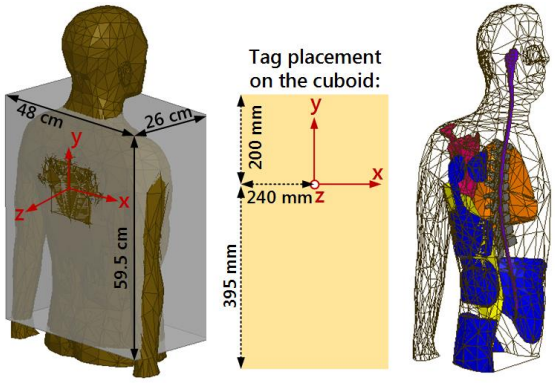

Fig. 2. Cuboid model visualised on top of the solid body model (left) and the transparent view of the structured body model (right). In the structured model, the material for the transparent part is skin. The red, dark grey, blue, yellow, and orange denote cortical bone (scapula), cancellous bone (thoracic vertebrae T3-T12), muscle, fat, and air (inside lungs), respectively.

that: $\mathbf{E}=\mathbf{E}_L+\mathbf{E}_R=\mathbf{E}_L+\gamma\mathbf{E}_L$ [10]. With this notion, the mutual polarisation loss factor between a tag antenna and incident wave from a reader with an arbitrary elliptic polarisation is

$$\chi_p=\frac{1+|\gamma_{inc}|^2|\gamma_{tag}|^2+2|\gamma_{inc}||\gamma_{tag}|\cos\Delta}{(1+|\gamma_{inc}|^2)(1+|\gamma_{tag}|^2)}, \quad (2)$$

where the complex scalars γ_{tag} and γ_{inc} are the circular polarisation ratios of the incident wave and the tag antenna, respectively, and Δ is the difference between the arguments of γ_{tag} and γ_{inc} [10]. Generally, RFID readers are equipped with circularly polarised antennas to eliminate the possibility of cross polarisation with tags that comprise almost invariably a linearly polarised antenna due the stringent requirements on size, cost, and manufacturing complexity. For the pure left and right hand circular polarisations, we have $\gamma_{inc}=0$ and $|\gamma_{inc}|\to\infty$, respectively. In these cases, equation (2) yields the mutual polarisation loss factors

$$\chi_{LH}=\frac{1}{1+|\gamma_{tag}|^2} \quad \text{and} \quad \chi_{RH}=\frac{1}{1+|\gamma_{ant}|^{-2}}. \quad (3)$$

For a perfectly linearly polarised tag antenna $\gamma_{ant}=1$ [10] and both loss factors in equation (3) become equal to 1/2.

For further analysis, we define the read range coverage C_α with $0<\alpha<1$, so that in α percentage of the spatial observation angles $C_\alpha<d_{tag}(\theta,\phi)$. This means that when an incident wave from the reader impinges upon the tag, there is an α percentage probability for detecting the tag at a distance longer than C_α.

We used ANSYS HFSS v15 in modelling the antennas. Firstly, Fig. 3 shows the simulated τ. According to our parametric study, it was not possible to achieve higher τ with the dipole constrained in the 20×

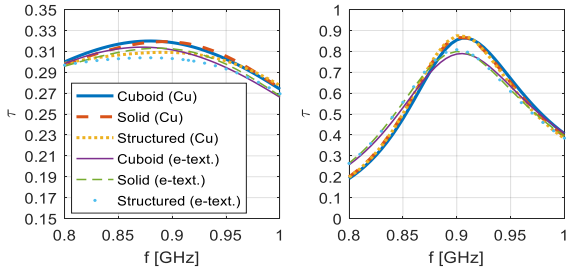

Fig. 3. Antenna-IC power transfer efficiency of the dipole (left) and folded dipole (right) tags.

Table 1: Radiation efficiency (%) and directivity (dBi) in the direction of the positive z-axis in Fig. 2.

	Dip., Cu	Dip., e-textile	Folded, Cu	Folded, e-textile
Cub.	1.8 %	1.7 %	1.2 %	1.0 %
	7.6 dBi	7.6 dBi	6.2 dBi	6.2 dBi
Solid	1.8 %	1.7 %	1.1 %	0.9 %
	7.5 dBi	7.5 dBi	7.3 dBi	7.3 dBi
Struct.	1.7 %	1.6 %	1.0 %	0.8 %
	7.4 dBi	7.4 dBi	7.3 dBi	7.3 dBi

120 mm^2 footprint size by optimising the embedded inductive matching loop (params.: *u* and *v*) due to the inherently elevated antenna resistance. This indicates that though widely applicable for tags in item level tracking applications, this impedance tuning approach has limited applicability in wearable tags. In contrast, we found that the folded dipole permitted good impedance matching within equal footprint area.

Overall, all the body models predicted very similar impedance matching, suggesting that a simplistic body model suffices for optimizing the antenna impedance. In addition, Table I shows that the radiation characteristics observed from the direction of the positive z-axis, are also very similar among all models, with the exception that the cuboid model predicted 1 dB lower directivity for the folded dipole compared with the anatomical models. Moreover, the antennas' radiation performance is characterised by low radiation efficiency in the order of 1% and high directivity – both due to the impact of the human body. The radiation patterns at other observation angles, however, differ notably between the cuboid and anatomical models as shown in Fig. 4. Consequently, the spatial coverage presented in Fig. 5 differs between these models suggesting that we need anatomically shaped models for the judicious analysis of the coverage and read range of wearable tags.

In the analysis of the spatial coverage, we assumed that a reader antenna may be located anywhere behind the person (θ = –90°…90°) within a 60° beam in the yz-plane (ϕ = –30°...30°). We discretised the ranges for θ and ϕ using steps of 2.5° and 1°, respectively, and

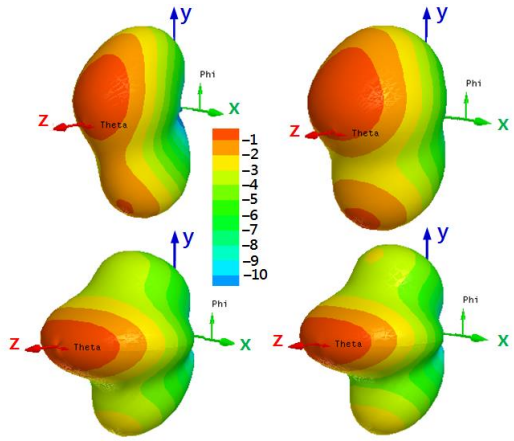

Fig. 4. Radiation patterns of the copper antennas in cuboid (top) and solid body models (bottom) at 915 MHz. Left dipole, right: folded dipole.

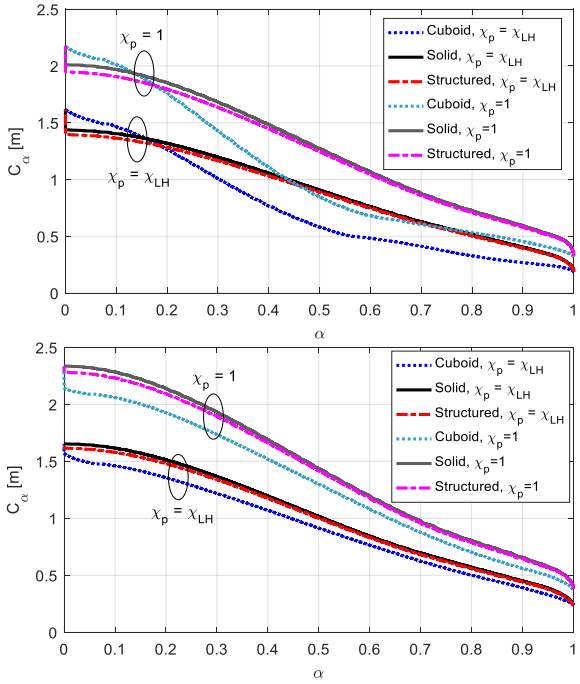

Fig. 5. Spatial coverage of the e-textile dipole (top) and e-textile folded dipole (bottom) at 915 MHz in the region where θ = –90°…90° and ϕ = –30°...30°.

extracted the directivity and left-hand circular polarisation ratio at each point. As shown in Fig. 5, the solid and structured anatomical models predicted nearly identical coverage, whereas the cuboid model yielded lower values. This is because the radiation patterns obtained from the anatomical models exhibit broader beams in the xz-plane (Fig. 4). Overall, in the anatomical models, the e-textile dipole and folded tags achieved the peak d_{tag} of approximately 2.0 m and 2.3 m in polarisation matched scenario and 1.4 m and 1.6 m in the case of a left-hand circularly polarised reader, respectively. The corresponding values of $C_{0.5}$ are 1.2 m

and 1.4 m for χ_p = 1 and 0.9 m and 1.0 m for $\chi_p = \chi_{LH}$. Hence, even though the maximum d_{tag} is sufficient for practical applications of wearable tags, the important observation from the analysis of the spatial coverage is that the reliability of the detection, especially with a commonly used circularly polarised reader antenna, may still limit the applicability of the tags.

III. RESULTS FROM TESTING

During testing, we affixed the tags on the skin in the upper back of a male test subject as described in Fig. 1 and tested them wirelessly using Voyantic Tagformance measurement system. It contains an RFID reader with an adjustable transmission frequency (0.8…1 GHz) and output power (up to 30 dBm) and provides the recording of the backscattered signal strength (down to −80 dBm) from the tag under test. During the test, we recorded the lowest continuous-wave transmission power at which a valid 16-bit random number from the tag was received as a response to the query command in ISO 18000-6C communication standard. In addition, the wireless channel from the reader antenna to the location of the tag under test was characterised using a system reference tag with known properties. As explained with details in [7], this enabled us to estimate the attainable read range of the tag. In the measurement, we used a linearly polarised reader antenna aligned for polarisation matching with the linearly polarised tags. Fig. 6 shows the results referred to *EIRP* = 3.28 W. The excellent agreement between the simulations and measurement adds assurance to the modelling approaches presented in the previous section.

IV. CONCLUSION

Wearable antennas couple electromagnetically to the human body making electromagnetic body models an indispensable tool for optimising them. We compared three different models for the torso: cuboid and anatomical models with and without internal structures, in the modelling of wearable RFID tags. We found little difference in antenna impedance obtained from the models, but the cuboid predicted notably different radiation pattern. Moreover, we found the difference in all performance indicators obtained from the solid and structured models negligible suggesting that the anatomical model without internal structures is the most effective one for our application.

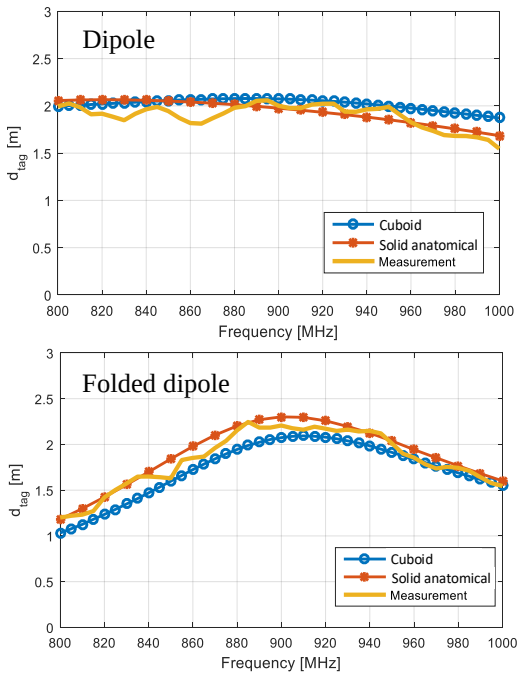

Fig. 6. Attainable read range toward +z-axis in Fig. 2.

REFERENCES

[1] J. M. Rabaey, "The human intranet—where swarms and humans meet," *IEEE Pervasive Comput.*, vol. 14, no. 1, pp. 78–83, Jan.–Mar. 2015.

[2] S. Lemey, F. Declercq, and H. Rogier, "Textile antennas as hybrid energy-harvesting platforms," *Proc. IEEE*, vol. 102, no. 11, pp. 1833–1857, Nov. 2014.

[3] A. Sani, M. Rajab, R. Forster, and Y. Hao, "Antennas and propagation of implanted RFIDs for pervasive healthcare applications," *Proc. IEEE*, vol. 98, no. 9, pp. 1648–1655, Sep. 2010.

[4] A. Yakovlev, S. Kim, and A. Poon, "Implantable biomedical devices: Wireless powering and communication," *IEEE Commun. Mag.*, vol. 50, no. 4, pp. 152–159, Apr. 2012.

[5] Z. Fu and F. Yang, "A slotted patch antenna integrated with thermal switch for high-sensitivity temperature monitoring," *IEEE Antennas Wireless Propag. Lett.*, vol. 14, pp. 998–1001, Jan. 2015.

[6] O. O. Rakibet, C. V. Rumens, J. C. Batchelor, and S. J. Holder, "Epidermal passive RFID strain sensor for assisted technologies," *IEEE Antennas Wireless Propag. Lett.*, vol. 13, pp. 814–817, Apr. 2014.

[7] F. Long, X. Zhang, T. Björninen, J. Virkki, L. Sydänheimo, Y.-C. Chan, and L. Ukkonen, "Implementation and wireless readout of passive UHF RFID strain sensor tags based on electro-textile antennas," in Proc. 2015 European Conf. Antennas Propag., 5 pages.

[8] X. Chen, L. Ukkonen, T. Björninen, and J. Virkki, "Comparison of e-textile dipole and folded dipole antennas for wearable passive UHF RFID tags," accepted in PIERS, 19–22 Nov. 2017, Singapore.

[9] IT'IS Fondation, Tissue Properties. Available: https://www.itis.ethz.ch/virtual-population/tissue-properties/downloads/

[10] T. A. Milligan: *Modern Antenna Design*, 2nd Ed., John-Wiley & Sons, Inc., 2005.